



Physical Mechanisms Based Constitutive Model of Creep in Irradiated and Unirradiated Metals at Cryogenic Temperatures

Aneta Ustrzycka*

Institute of Fundamental Technological Research, Polish Academy of Sciences, Poland



ARTICLE INFO

Article history:

Received 6 October 2020

Revised 6 January 2021

Accepted 27 January 2021

Available online 2 February 2021

Keywords:

Creep in the proximity of absolute zero

Irradiation creep

Quantum-mechanical tunneling effect

Cryogenic temperatures

Low thermal energy

Peierls stress hills

ABSTRACT

The present work describes the physical mechanisms of low temperature creep in irradiated and unirradiated metals. The slow inelastic deformations of solids under stress below the yield stress of the material are considered. For the problem of creep at cryogenic temperatures, the classical creep models are not enough. The purpose of this paper is to formulate a physically-based constitutive model of creep for irradiated materials at cryogenic temperatures (liquid nitrogen 77 K, liquid helium, 4.2 K) based on the idea that a dislocation held up by a potential barrier can pass through it owing to the quantum-mechanical tunnelling effect. The problem is novel in the context of recognition of physical mechanisms taking place at cryogenic temperatures leading to the evolution of radiation induced defects under mechanical loads. Creep produced by the expansion of irradiation induced dislocation loops is considered. The kinetic law for evolution of a dislocation loop is proposed using the mechanism of development of a dislocation line over Peierls stress hills. Also, creep produced by the elastic interaction of a radiation induced point defects with existing dislocations in materials is regarded. Predicted creep rate behaviour as a function of stresses and dpa are presented which would need to be validated with data in irradiated materials. Moreover, the new constitutive model of low temperature creep in unirradiated materials is formulated. The Glen-Mott quantum mechanical dislocation tunnelling effect allows extending the theory to the liquid helium temperature range. For this case of unirradiated materials, the creep curves validated experimentally for copper and stainless steel in cryogenic temperature are shown.

© 2021 The Author(s). Published by Elsevier B.V.

This is an open access article under the CC BY license (<http://creativecommons.org/licenses/by/4.0/>)

1. Introduction

Low-temperature creep can be observed in many scientific instruments connected to electronic, space and nuclear industries. Metal and alloys used in cryogenic applications and additionally subjected to irradiation show superior physical and mechanical properties, also ductility. These materials cooled to cryogenic temperatures, nearly down to the temperature of absolute zero, subjected to constant stress amplitude during operation in the pre-yield regime may undergo time-dependent deformations that affect the intended performance. Contrary to popular belief, the creep phenomenon that leads to nonrecoverable deformation during a material lifetime might cause significant problems for applications. For this reason, the creep mechanism in irradiated and unirradiated materials at extremely low temperatures (liquid nitrogen 77 K, liquid helium, 4.2 K) should be explained. Physical processes realised at cryogenic temperatures are characterised by

the weakly excited lattice and lack of thermal energy. Experimental results carried out at extremely low temperatures (liquid nitrogen 77K and liquid helium 4.2K) indicate that creep deformations are observed immediately after applying loads [22,35]. Depending on the applied stress, the creep deformations cause failure of the structural components even at low temperatures. For the problem of creep at cryogenic temperature, classical creep models for elevated temperatures range are not enough. The literature data [2,13,19,23,24] show that the creep rates extrapolated from elevated to extremely low temperatures are smaller even by several orders of magnitude. In fact, the creep rates at extremely low temperatures are only one or two orders of magnitude smaller than the creep rates at elevated temperature. Activation energy changes indicate the mechanism changes for creep, so creep at cryogenic temperatures cannot be predicted by extrapolation from higher temperatures. The physical mechanisms of creep at extremely low temperatures are not yet fully established. The quantum mechanical dislocation tunneling was first considered by Glen [7] and Mott [17] who considered the possibility of moving low activation energy dislocation through the energy barriers as a consequence of quantum phenomena. Weertman [34] has proposed

* Corresponding author.

E-mail address: austrzyc@ippt.pan.pl

a low-temperature dislocation creep model to account for the creep activation energies. Weertman [34] has also considered tunneling through a Peierls potential. This paper provides a wealth of interesting analysis of the tunneling dislocation motion. In addition, Gilman [6] determined the tunneling probability of dislocation motion. The temperature dependence of the process and phonon-assisted tunneling are also discussed.

In this paper, the physically based constitutive models of creep at extremely low temperature in irradiated and unirradiated metals are proposed. The creep mechanism is based on the hypothesis that dislocations can pass through energy barriers due to the Glen-Mott quantum-mechanical tunneling effect. At low temperatures stress-activated nonrecoverable deformation occurs in solids. The constitutive relation for the activation energy and the stress required to force a dislocation through the obstacles without the help of temperature is adopted. The creep curves validated experimentally for copper and stainless steel in cryogenic temperature are shown. It is shown, that the creep rate determined by the tunneling effect is in a good agreement with experiment. In this paper, the first formulation of constitutive model of creep at extremely low temperature in irradiated materials is proposed. The constitutive model is based on the experimental estimation of concentration of radiation induced defects (interstitials, interstitial clusters, vacancies, vacancy clusters, dislocation loops) in stainless steel as a function of radiation damage dpa (displacement per atom). The total creep rate is expressed by the respective components corresponding to relevant physical mechanisms responsible for the irradiation creep behaviour. The first term corresponds to the creep resulting from nucleation of dislocation loops and their expansion under the mechanical loads. The relevant kinetics of evolution of radiation induced dislocation loop under mechanical loads is formulated. The second term arises from the effect of stress on the elastic interaction of a radiation induced point defects with existing material dislocations. The kinetic law of motion of a dislocation segment under applied stress is proposed using the mechanism of development of a dislocation line over Peierls stress hills. The last term results from swelling. Predicted creep rate behaviour produced by the expansion of irradiation induced dislocation loops is shown.

2. Physical behavior of irradiated and unirradiated metals at low temperatures

2.1. Near 0 K thermodynamic instability

The cryogenic involves a wide range of achievable temperatures. It is a very interesting issue due to the large number of physical phenomena that occur within it. It is worth mentioning a few of that such as quantum effects, superconductivity and superfluidity and solid-state phase transformations. In applications of cryogenics liquefied gases like liquid helium (4.2 K) and liquid nitrogen (77 K) are commonly used. At extremely low temperature physical behavior and properties of material completely changes. Thermodynamic principles have a fundamental meaning for cryogenic temperatures and constitute the basis for the explanation of physical mechanisms responsible for the behavior of metals during creep at these temperatures.

For cryogenics, heat capacity defined in terms of derivative of either the entropy or internal energy is a fundamental state property of matter. Furthermore, heat capacity is associated with the specific heat, transient heat transfer, and thermal energy stored. In order to describe the behavior of metals at extremely low temperature it is assumed that the heat transport in the lattice is based on the phonon mechanism and the free electrons. In the case of solids, the phonon contribution to the heat capacity dominates.

However, the thermal conductivity connected with transport properties at low temperatures is much smaller because the phonon transport is less effective than electron transport. Additionally, in the range of cryogenic temperatures a thermal contraction resulting from a change in physical dimension of materials is observed. It can be a big influence on the design of engineering devices, largely because the thermal contractions of different materials vary considerably. An interesting phenomenon occurring at low temperatures is certainly superconductivity, state with essentially zero electrical resistance. With the discovery of high-field superconductive materials, technical applications have come to fruition. In particular, superconductive magnets and superconductive electronics are now fairly well-established applied subfields of superconductivity. The mechanical properties of materials are of considerable importance in the design of cryogenic systems and enter into calculations of failure modes in mechanical structures (see [26,30]).

2.2. Interaction of radiation with matter at low temperatures

In order to investigate the irradiation creep problem the main processes that underlie the response of the irradiated material to stress should be recognized. The processes of the defect formation and initial clustering, as well as the interaction between point defects which are the basis of the creep theory, should be considered. The processes are made up of several stages. The following considerations are carried out on the solids in which the atom locations are defined by the crystalline structure. The irradiation of metals by high energy particles leads to an interaction of energetic incident particles with lattice atoms. Exposure to irradiation (flux of particles) implies creation of clusters of defects in the material. A beam of high energy particles is supposed to eject the atoms from their thermodynamic equilibrium positions in the lattice and move them to other places. Interstitials and vacancies are created (Fig. 1).

The energetic particles transfer their kinetic energy to the lattice atoms creating primary knock on atom (PKA), which, in turn, leads to the displacement of next generation of target atoms, the process is called collision cascade, [12,21].

As a direct result of the displacement process, and without any need for point-defect diffusion, the point defects form clusters, with the vacancies and interstitials condensing. Collision cascade usually contains a vacancy-rich core surrounded by a halo of interstitial atoms. Osetsky [23]. Displacement phase of the collision cascade usually lasts about 10^{-11} seconds, after about 10^{-10} seconds the cascade is thermalized. Temperature has a very strong impact on the clustering process. At higher temperatures, the recombina-

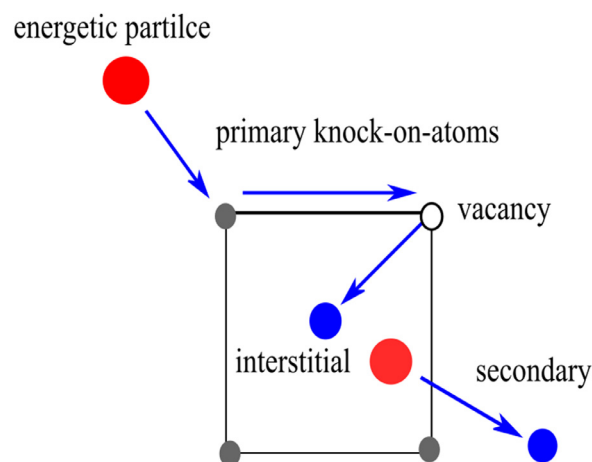


Fig. 1. Interaction of radiation with matter.

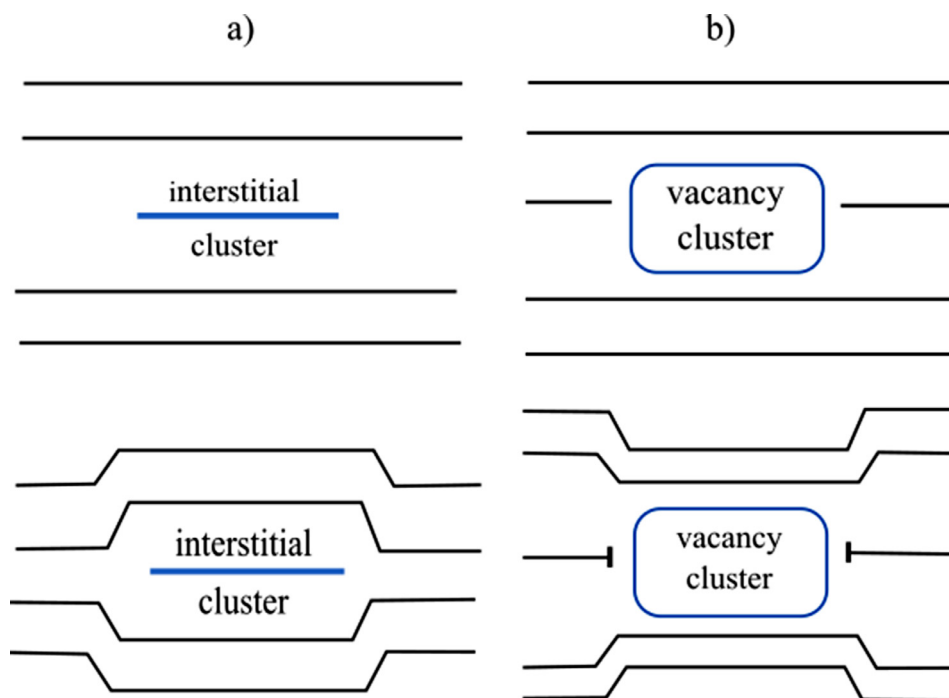


Fig. 2. Formation of irradiation induced dislocation loops a) interstitial loop b) vacancy loop.

tion process is observed and as a result the number of clusters is reduced. At extremely low temperatures only limited recombination takes place and a large fraction of micro-damage remains in the lattice [15]. The process of formation of irradiation induced dislocation loops is shown in Fig. 2.

Often vacancy clusters collapse to form vacancy loops at the site of the cascade (Fig. 2a). On the other side, the scattered interstitials nucleate interstitial loops (Fig. 2b). Interactions of dislocations with interstitials are more common. For this reason, interstitial loops tend to grow but vacancy loops tend to shrink and have a limited lifetime [16]. These phenomena such as point defects (vacancies and interstitials) and dislocation loops formation are characteristic for irradiated materials and determine the physical effects, and with the application of stress, the mechanical effects of irradiation.

2.3. Significance and assessment of low temperature creep

The evaluation of damage generated in solids subjected to irradiation is a major challenge in many technological domains connected to electronic, space and nuclear industries. Mathematical description of the thermo-mechanical property changes of materials during irradiation has fundamental meaning for the design of structures operating in extreme conditions: nuclear reactor, components of superconducting magnets, cryogenic lines in the particle accelerators, research and diagnostics instruments. There is a need to understand how electronics and communications equipment performs in space, under irradiation and at cryogenic temperatures. In space, spacecraft, satellite and deep space probe as well as electronics equipment and communications equipment are placed in an extremely harsh environment. They are subjected to temperatures near absolute zero, different levels of heightened irradiation and mechanical loads. These varying conditions cause different types and amounts of damage to the material. The crucial role of material behavior in the unique radiation environment makes the constitutive modelling of irradiation effect on mechanical properties of the materials at extremely low temperatures a subject of high importance. The problem is novel in the context of

combination of physical mechanisms of nano/micro damage generation in the lattice by a flux of particles and its further evolution under mechanical loads at cryogenic temperatures.

3. Experimental evidence of low temperature creep

3.1. Low temperature creep in copper

The creep behaviour of copper at the temperature of liquid helium (4.2 K) and liquid nitrogen (77 K) is exhaustively described based on the provided experimental tests by Yen et al. [35]. The creep strain curves as a function of time at extremely low temperature are illustrated in Fig. 3.

The creep tests were conducted with the loads $\sigma_1=20.7$, $\sigma_2=34.5$ $\sigma_3=48.3$ MPa and $\sigma_4=62.1$ MPa for periods up to 200 h. The tensile properties of copper at low temperatures are determined by Yen et al. [35]. The yield strength at low temperature 4.2 K is 38.5 MPa. The tensile properties of copper at 77 K are similar to that at 4.2 K. The creep strain level strongly depends on the stress level and temperature. For the higher value of stress the creep strain increases. In particular, the strain measured in Cu after 100 h, under the stress of around 60 MPa is about 10 times larger than for 20 MPa at the same temperature. Whereas, the creep strain at 4.2 K is more than three times smaller than at 77 K [35]. The primary creep stage is evident observed directly after loading, for all stress levels, at two temperature levels. The creep curves indicate that the length of the primary creep stage elongates and the primary creep strain increase with the increasing loads. Steady-state creep rate of annealed copper was determined during the period longer than 130 hrs for three levels of loads, 20.7 MPa, 34.5 MPa and 48.3 MPa. The experimental data and the extrapolations for the temperatures: 477 K and 77 K are presented in Fig. 4.

The steady-state creep rate in liquid nitrogen (77 K) reaches about 10^{-11} 1/s and increases with the increasing loads both for intermediate (477 K) and low temperature (77 K). It is worth pointing out, that the creep rates at low temperatures reach the values smaller only by one order of magnitude than the creep rates at the

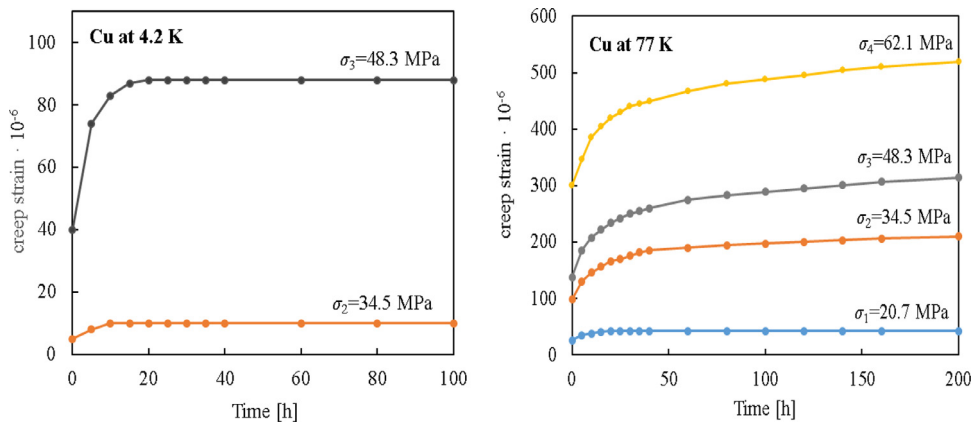


Fig. 3. Creep strain as a function of time for copper at 4.2 K and 77 K (after [35]).

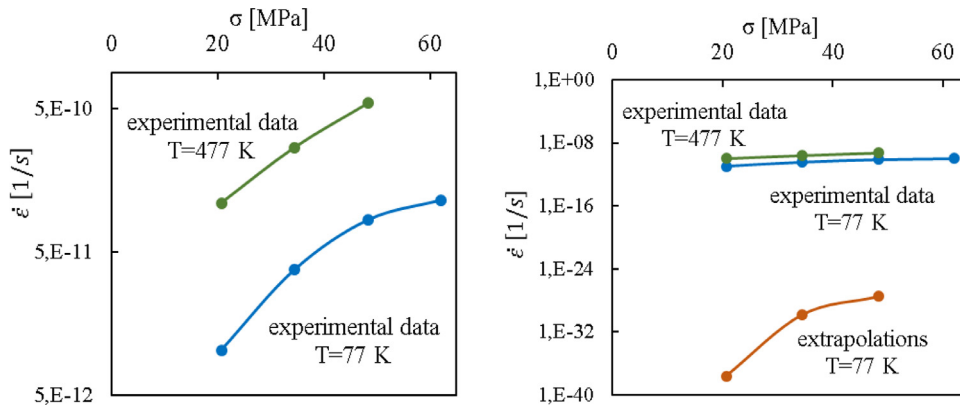


Fig. 4. Steady-state creep rate of annealed copper as a function of stress for 477 K and 77 K obtained from experimental data and extrapolations (after [35]).

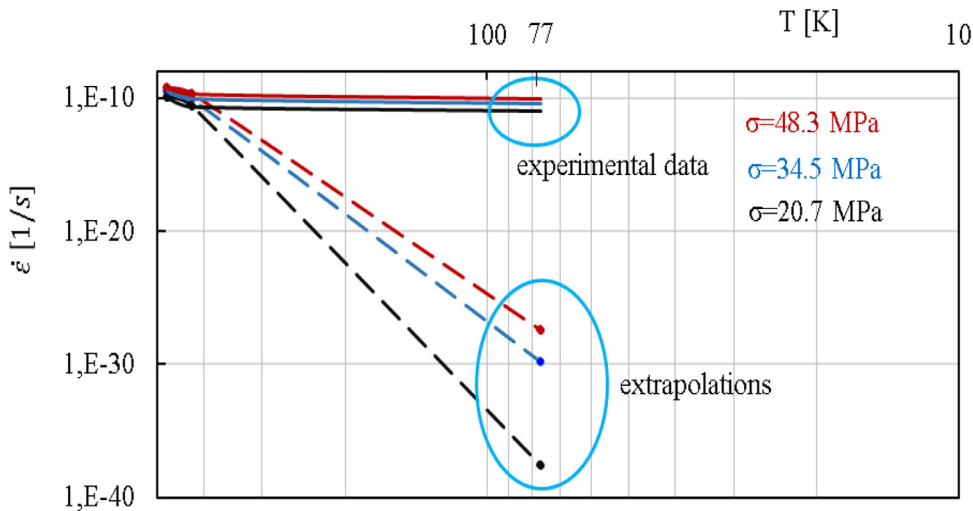


Fig. 5. Steady-state creep rate of annealed copper as a function of temperature obtained from experimental data and extrapolations (after [35]).

intermediate temperature. Therefore, this is not possible to neglect this phenomenon. For comparison, the extrapolated creep rates from intermediate temperature based on constant activation energy and the creep rates obtained from experimental data at cryogenic temperatures are shown in Fig. 5. The experimental results indicate that the creep rates obtained from experimental data remain much higher than the creep rates obtained from the extrapolation. Such huge disagreement indicates that another mechanism of creep deformation takes place at the extremely low temperatures. The steady-state creep rate of annealed copper as a func-

tion of temperature obtained from experimental data and extrapolations are presented in Fig. 5 after [35].

The slope change of the creep rate curves indicates the different mechanisms of the activation energy for creep at intermediate and low temperatures.

3.2. Low temperature creep in stainless steel

Stainless steels are extensively used in the industrial applications of extremely low temperature due to the possibility to

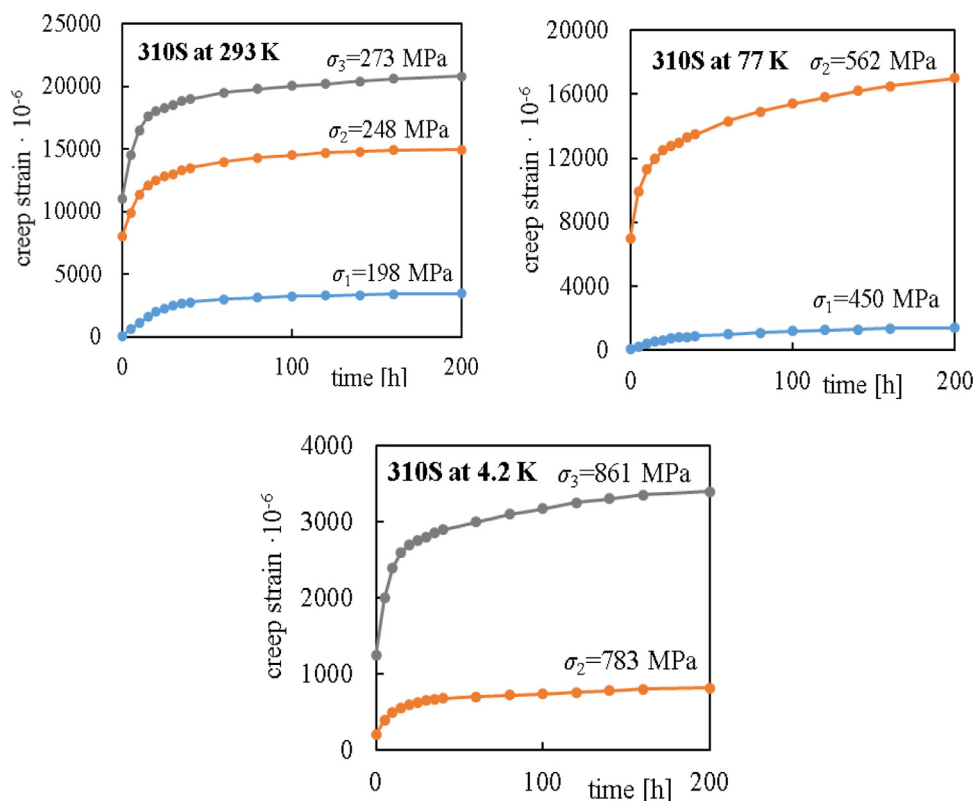


Fig. 6. Creep strain as a function of time for stainless steel 310S at 293 K, 77 K and 4.2 K (after [22]).

sustain high stresses under elastic conditions. For example, the components of superconducting magnets, cryogenic lines in the particle accelerators and coil cases of pool-cooled superconducting magnets for fusion reactors are made from stainless steels. Given the higher level of the yield stress of stainless steels when compared to copper, the creep tests are essentially performed at much higher stress levels. Creep strain curves for stainless steel 310S as a function of time at liquid helium temperature (4 K), liquid nitrogen temperature (77 K), and room temperature (293 K) are presented in Fig. 6 after Ogata et al. [22]. Tensile tests were performed at selected stress levels. The yield strength at each temperature level was determined by Ogata et al. [22]: $\sigma_0=248$ MPa at $T=293$ K; $\sigma_0=562$ MPa at $T=77$ K and $\sigma_0=783$ MPa at $T=4$ K.

The creep strain increased with the stress levels in all cases. Steady state creep rates, measured after 200 h at the level of yield stress are of the order of $14 \cdot 10^{-10}$ 1/s at 293 K and $0.83 \cdot 10^{-10}$ 1/s at 4.2 K. This entails that the creep rate for stainless steel 310S at liquid helium temperature (4.2 K) reaches significant values. Therefore it must be included during the design phase of construction elements working in liquid helium. However, 20% below the yield stress, the steady state creep rate at 4.2 K is practically equal to zero.

4. Physical mechanisms of creep deformation in metals at extremely low temperatures

Material hold at stress below yield stress for very short time undergoes only elastic deformation, in case of long periods inelastic deformation can occur by creep. Thus, creep is understood as a temperature sensitive time-dependent nonrecoverable deformation developing under the stress smaller than the yield stress. In general, deformation during a creep process results from diffusion flow, transport of the matter by the motion of thermal formation of vacancies and atomic diffusion. Alternative creep mechanisms

are the dislocation climb over obstacles, dislocation glide along the slip plane and the dislocation cross-slip [1,4,8]. Due to appearing stress fields in the material, dislocations can interact with each other, with foreign atoms and impurity defects. These interactions are the main physical mechanisms for creep. Creep is essentially a temperature dependence process. The probability of dislocations motion or formation of vacancies has a strong dependence on the activation energy. Increase of temperature leads to accumulation of the thermal energy required to trigger the proper creep mechanism. On the other hand, creep is also dependent on the applied stress to the material [28,29,36]. The stress level obtained inside material is a decisive factor for activation of the appropriate creep mechanism.

Radiation significantly increases the creep rate in comparison to the creep rate induced by thermal creep or creep induced by other possible mechanisms. Radiation leads to creation of point defects in the solid whereas irradiation creep causes the evolution of microstructure by the interactions between interstitials, vacancies and dislocation loops produced by the radiation and atoms in the lattice structures. The effect of increase radiation induced damage causes only minimal acceleration of thermal creep, it also does not increase diffusional creep rate. Rather, irradiation creep can be understood as a process leading to evolution of radiation damage microstructure in metals under the applied stress. Radiation can also lead to nucleation of dislocation and the bowing of existing dislocation lines by absorption of defects [20]. The process of radiation induced defects absorption depends on their orientation with respect to the external stress and afterwards it causes a microscopic creep strain [33]. Another deformation mechanism activated creep, swelling is understood to be the climb and glide mechanism due to the absorption of interstitials on dislocations unassisted by stress. This process causes swelling of the irradiated solids due to the precipitation of gas bubbles. Irradiated materials eventually become highly porous and internal pressure develops Ustrzycka et al.

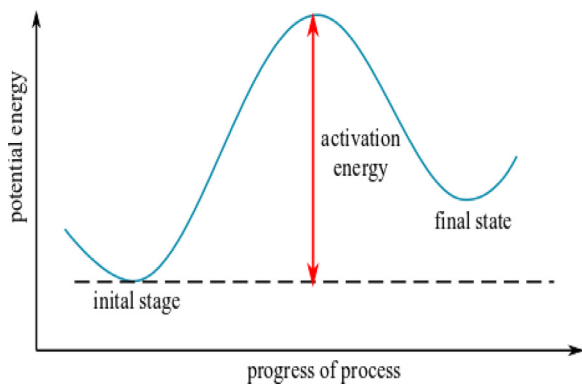


Fig. 7. Activation energy plotted against the progress of the process.

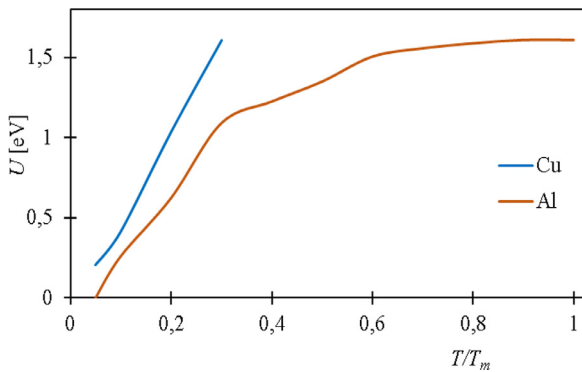


Fig. 8. The activation energy for steady-state deformation creep of Cu and Al as a function of temperature (after [14] and [9] and [11]).

[27,32]. It is worth pointing out, that under irradiation, there is the possible deformation that is "geometric" and/or volumetric in nature, unlike the thermal and stress induced creep.

4.1. Thermal activation during creep

The mechanisms of creep deformation in metals at cryogenic temperatures are generally based on an activation energy U . The activation energy is understood as the energy which should be introduced into the system in order to activate a physical phenomenon. Activation energy can be thought of as the magnitude of the potential or energy barrier (Fig. 7).

At elevated temperatures, the activation energy U can be calculated based on the Arrhenius type creep rate equation

$$\dot{\epsilon}^c = -A \left(\frac{\sigma}{E} \right)^n \exp \left(\frac{-U}{RT} \right) \quad (1)$$

Knowing the ratio σ/E , the activation energy U for steady-state creep rate can be expressed in the following form

$$U = -R \left(\frac{\partial \ln \dot{\epsilon}^c}{\partial \left(\frac{1}{T} \right)} \right) \Big|_{\sigma/E} \quad (2)$$

The activation energy for steady-state deformation creep of Cu and Al as a function of temperature is presented in Fig. 8. It should be noted, that that the activation energy dramatically decreases for the temperatures lower than $0.3T_m$, where T_m denotes the melting temperature. The values of activation energy are much lower than at higher temperatures, where the mechanism of creep deformation is associated with dislocations creep or dislocations climb.

The change in the activation energy at lower temperatures indicates a change in the creep mechanism. Different creep mechanism than the dislocations climb is activated.

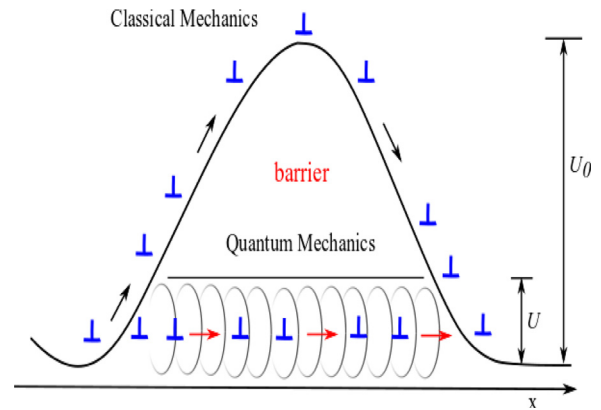


Fig. 9. Classical (over the barrier) motion vs. quantum (through the barrier) mechanical tunneling of dislocations.

Thus, the activation energy must change for creep to occur at cryogenic temperatures, which has been experimentally confirmed.

4.2. Quantum-mechanical tunneling of dislocations

The purpose of this paper is to explain the creep mechanism at low temperatures, based on the idea that a dislocation can pass through the potential barrier due to the quantum-mechanical tunneling effect. Fig. 9 shows a schematic model of a classical motion vs. quantum mechanical tunneling of dislocations. In the context of classical mechanics, the dislocations with energy higher or equal to potential energy barrier U_0 reach the final state by passing over the barrier. In the case of the smaller activation energy than U_0 , the dislocations collide and glance off the barrier. Thus, according to classical mechanics controlled by the law of conservation of energy, dislocations must climb the potential barrier to appear on the other side of the barrier. In the framework of quantum mechanics since all dislocations have a wave character, the dislocations with energy U can pass through the barrier due to mechanical tunneling of dislocations, x represents distance measured in the direction of motion of the particle.

The proposed mechanism of quantum tunneling of dislocations to explain the creep process at very low temperature enables a completely new dynamics of dislocations due to their wave properties. It should be noted that the mechanisms offered by classical mechanics are completely blocked at extremely low temperatures. Quantum mechanical tunneling of dislocations opens the new opportunity to set in motion the dislocations at the temperature of liquid nitrogen and helium. Quantum mechanics allows dislocation with less energy to tunnel through the barrier even if its energy is less than the potential energy of the barrier.

4.3. Peierls lattice resistance mechanism

The other mechanism responsible for creep in solids is connected with the Peierls stress field. This mechanism is realised by the motion of dislocations by overcoming the periodic lattice resistance in solids. Peierls stress is the stress required to overcome the periodic potential barrier on the slip plane. In this case, the dislocation is moving in a Peierls potential which is characterised by hills and valleys of potential energy. During this process the Peierls stress hills control the dislocation motion. This mechanism allows dislocations to move to overcome the Peierls potential after expansion under the stress of a jog in. Dislocation line located in the place of minimum potential energy is thrown over Peierls hill into the following Peierls valley. If the Peierls stress is impossible to achieve, dislocation lines move along determined crystallographic

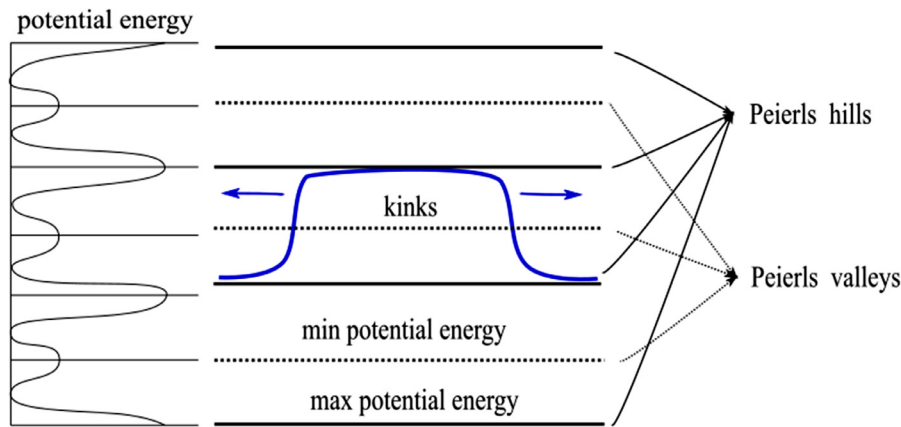


Fig. 10. Double-kink of a dislocation line by overcoming Peierls potential.

directions. The overcoming the Peierls stress is a necessary condition to move a dislocation line one atomic distance. The motion of dislocation by overcoming Peierls potential is shown in Fig. 10.

Initially, the dislocation line is located along a crystallographic direction (slip system). Under the action of an applied stress double-kink moves a short section of dislocation line over to the next equilibrium position with the minimum potential energy. Then, the broke short section of dislocation line will be moved apart under the applied stress until the whole dislocation line has moved an atomic distance. In the next step, under the applied stress the displaced short section of dislocation line will be moved apart even more until the whole dislocation line has moved an atomic distance. An expression that specifies the minimum energy U needed to run the process has been proposed by Seeger et al. [25] in the form

$$U = E_k \left(1 + \frac{0.25 \ln 16 \sigma_p}{\pi \tau} \right) \quad (3)$$

where E_k is the kink energy of dislocations, σ_p denotes the Peierls stress and τ is the resolved shear stress. This mechanism based on the Peierls potential has been observed experimentally for the low temperature (1.4 to 76 K) nonrecoverable deformation of metals by Koval et al. [13]. This mechanism is characterized by low activation energy, the kink energy was estimated based on the internal friction study (0.04 eV) and it was confirmed experimentally. Furthermore, the mechanism connected with Peierls stress is characterised by small activation volume equal to approx. $10b^2$. The length of dislocation segment is equal to ten times of Burgers vector b . Based on the experimental results for copper Koval et al. [13] concluded that steady-state creep is controlled by the mechanism based on the Peierls potential. In the other paper, presented by Tien and Yen [31] has shown that dislocation mechanism is responsible for transient creep. The above analysis has shown that mechanism based on the Peierls potential can become rate-controlling in metals during the secondary stage after a dislocation mechanism associated with mobile dislocations interactions has been completed. However, it is imperative to conduct long-term testing for a complete understanding of cryogenic creep behavior of materials.

The velocity of motion of a dislocation segment under applied stress smaller than the Peierls stress has been calculated by Seeger [25]

$$\frac{dx}{dt} = \frac{\nu La}{b} \exp\left(-\frac{U}{kT}\right) \exp\left(\frac{\pi \sigma U}{2 \sigma_p kT}\right) \quad (4)$$

where ν denotes the frequency of vibration of a dislocation line, L is a length of dislocation segment, a is the distance between Peierls hills, k is Boltzmann's constant, and T is the absolute temperature.

The L/b term comes in because there are many ways of creating the two jogs in a segment of length L . It is worth pointing that at a low-stress state velocity of motion of dislocation segment is independent of stress.

5. Constitutive modelling of low temperature creep

5.1. Model of quantum-mechanical dislocation tunneling

The activation energy observed for dislocation motion during low-temperature creep is temperature independent. Low temperature creep experiments show that in the liquid helium temperature range stress-activated creep deformation occurs in solids [22,35]. The theory of creep at extremely low temperatures is based on the Glen-Mott quantum-mechanical dislocation tunneling effect [17]. The dislocations not thermally activated can pass through an energy barrier because of the quantum-mechanical tunneling effect. The possibility of the tunnel effect arises from the fact that the energy barrier becomes low and narrow when applied stress approaches the stress required to force a dislocation through the obstacles. Following Glen's and Mott's suggestion one assumes that activation energy to form a jog, and thus to pull a dislocation through a barrier is given in the following form

$$U = U_0 \left(1 - \frac{\sigma}{\sigma_0} \right)^{3/2} \quad (5)$$

where σ denotes the stress acting on the dislocation and σ_0 is the stress required to force a dislocation through the obstacles without the help of temperature, U_0 denotes the jog energy. The distribution of stress-dependent activation energy U as a function of stress is shown in Fig. 11 for two types of materials (stainless steel and copper) at 7 K and 77 K. The value of creep activation energy U_0 for copper at the temperature of liquid nitrogen (77 K) was estimated by Yen et al. [35] at around 0.02 eV. The typical level of activation energy was obtained from a plot of $\ln \dot{\epsilon}$ versus the reciprocal inverse of the absolute temperature (see [35]). This is two orders of magnitude less than the activation energy measured in copper at elevated temperatures. Similar results were obtained for stainless steel.

These differences in creep activation energy values at cryogenic and elevated temperatures indicate differences in the dislocation dynamics between the cryogenic and the enhanced temperatures. The increased barrier height is expressed by a simple function dependent on the applied stress

$$W = W_0 \left(1 - \frac{\sigma}{\sigma_0} \right)^{3/2} \quad (6)$$

where W_0 is of order a few electron volts.

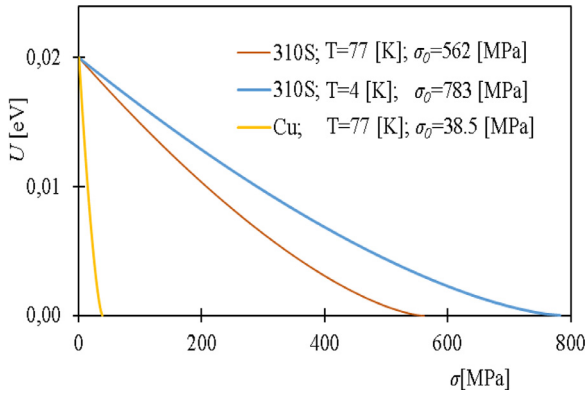


Fig. 11. The activation energy for 310S and Cu as a function of stress at 4K and 77 K.

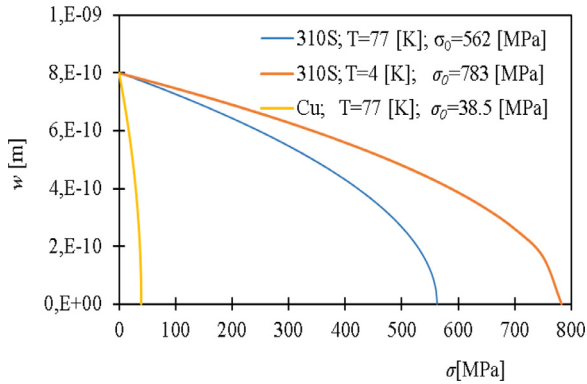


Fig. 12. Width of the potential barrier as a function of stress for 310S and Cu at 4K and 77 K.

Width of the barrier reads

$$w = a \left(1 - \frac{\sigma}{\sigma_0}\right)^{1/2} \quad (7)$$

where a is of the order of an interatomic distance.

The distribution of the width of the potential barrier as a function of stress for 310S at 77 K is shown in Fig. 12. The nature of the curves shows a strong dependence on the σ_0 dislocation unpinning stress.

The purpose of the present discussion is to show that tunneling can account for stress-activated flow. This implies that conventional thermal-activation models are often inappropriate, although they become appropriate when the temperature is high and the local internal stress is low. When quantum tunneling mechanism is responsible for creep deformation the temperature-dependent term should be replaced by the term expressed the tunneling probability.

Gilman [6] derived the probability of tunneling as

$$P = \exp\left(\frac{-mH_0^2}{4\hbar^2\sigma b}\right) \quad (8)$$

where σ denotes applied stress, m is an effective mass of moving dislocation (atomic mass per atomic plane cut by it [17]), H_0 is the total binding energy per unit length of dislocation, μ is the shear modulus and b denotes Burgers vector. Gilman [6] further simplified Eq. (8) by using several assumptions and approximations giving the following simplification for the tunneling probability

$$P = \exp\left(\frac{-\beta\mu}{\sigma}\right) \quad (9)$$

where β is a coefficient determined from experiments. Eq. (9) indicates that the tunneling probability, and hence the rate of stress-activated flow, is a very strong function of the applied stress. For

the sake of completeness, Gilman's derivation of the probability of quantum tunneling of dislocation motion in Appendix is provided.

In the regime where quantum mechanical dislocation tunneling is important, the tunneling process can be phonon-assisted which creates a special form of temperature dependence because phonons exhibit tunneling behavior where heat can be transferred via phonons.

5.2. Dislocation loops creep model

A low-temperature dislocation loops creep model was proposed by Weertman [34] to account for the creep activation energies. The proposed model allows formulating a general constitutive equation for transient and stationary creep.

The theory proposed by Weertman [34] is applicable under easy glide conditions where the spacing of the dislocations remains constant but should not be used when double glide occurs and the spacing of the dislocations becomes small. One would expect that in this case dislocation intersections are an important mechanism. In the Weertman approach the creep deformation is generated by the expansion of dislocation loops created at the Frank-Read dislocation sources. The creep rate is given in the following form

$$\dot{\epsilon} = b\pi\rho(\sigma_{eff})v_dR^2 \quad (10)$$

where v_d is the rate of dislocations production, R denotes the average radius to which a dislocation loop expands, and $\rho(\sigma_{eff})$ is the density of sources active at effective stress. An effective stress σ_{eff} means as applied stress minus the internal stress. The stress necessary to activate a dislocation source of length L is expressed in the form of a known phenomenological equation

$$\sigma = \frac{b\mu}{L} + \sigma_d + h_e \quad (11)$$

where h_e is the hardening stress caused by dislocations and point defects created during deformation, σ_d is constant stress which arises from point defects and dislocations present before deformation, and μ is a shear modulus. The first term in Eq. (11) is equivalent to the stress needed to activate a source of length L in the absence of internal stresses.

Here the spacing of the dislocation forest is L which is smaller than the length of the source. The loop can be expanded through the forest only if the effective stress is raised to a value of the order of $\mu b/L$. Weertman [34] analysis showed that the expansion of the dislocation loop is not possible if the spacing of the dislocation forest is smaller than the source length. Fig. 13 shows the dislocation loop created at a source of length L' unable to move through a forest of spacing L . In the present case, the stress level is sufficient only to activate the source and is not sufficient to activate the dislocation loops without the aid of thermal stresses. There is possible the evolution of the dislocation loop if the spacing of the forest in the immediate neighbourhood of the source is of the same dimension or larger as the source. Fig. 13 shows the forest spacing L' equals the source of length out to a distance L^* , beyond which the forest spacing returns to the value of L . At a stress level of $\mu b/L'$ the dislocation loop can evolve to the radius L^* .

Fig. 14 shows a schematic plot of the distribution of the density of sources. At effective stress $\sigma_{eff} = \mu b/L$ practically all of the sources are activated. At stress $\sigma_{eff} = \beta\mu b/L$, where β is a constant fraction, only a few numbers of sources are active.

The function of distribution of the density of sources $\rho(\sigma_{eff})$ can be obtained experimentally from observations of dislocation networks. The rate of expansion of a dislocation loop of radius r is calculated from Weertman's theory [34] and takes the form

$$\dot{r} = \frac{vra}{b} \exp\left(\frac{-U}{kT}\right) \quad (12)$$

where a is the distance between Peierls hills.

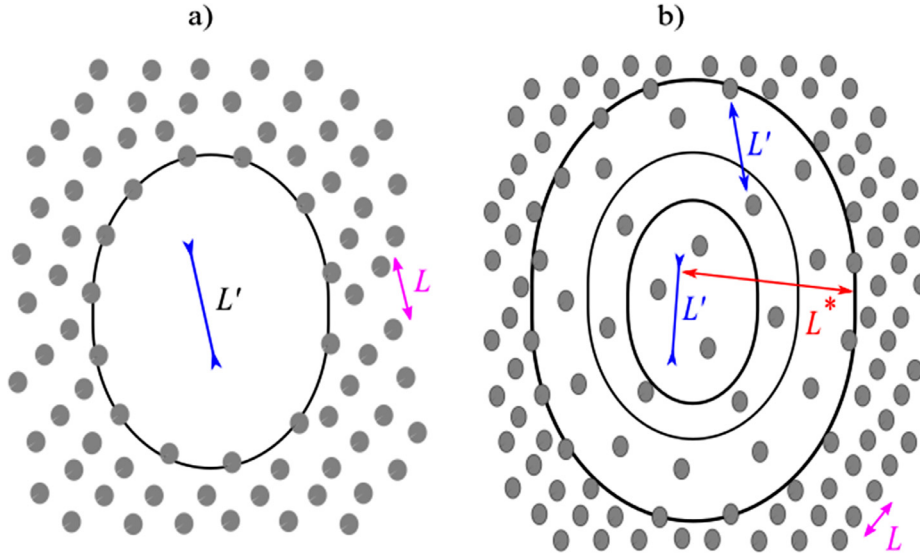


Fig. 13. a) Dislocations loop created at a source of length L' , b) Dislocation loop expanded through the forest of spacing L' out to a radius of L^* .

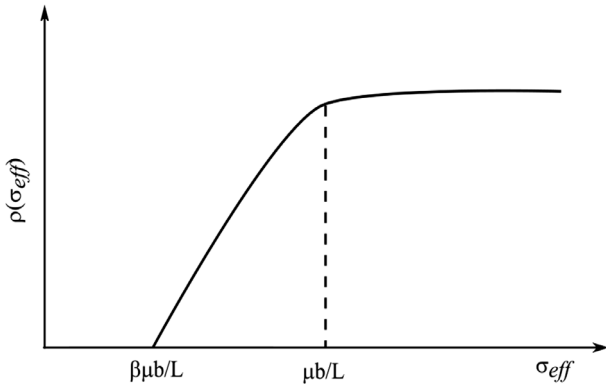


Fig. 14. Number of sources with expandable loops activated at different stress levels.

According to Weertman's theory [34] the activation energy U is expressed as a function of the Peierls stress

$$U = \frac{4ab}{\pi} \sqrt{\frac{2\mu\sigma_p ab}{5\pi}} \quad (13)$$

The frequency of vibration of a dislocation line ν is expressed in the form

$$\nu = \frac{\nu_t}{a} \sqrt{\frac{5\mu\sigma_p}{2\mu b}} \quad (14)$$

where ν_t is the velocity of shear waves in the metal.

Since R is approximately $\dot{\gamma}/L$, including Eq. (12) one obtains

$$R = \frac{\nu a}{b} \exp\left(\frac{-U}{kT}\right) \quad (15)$$

Finally, the creep rate is expressed in the following form

$$\dot{\epsilon} = \pi \nu a R^2 \rho(\sigma_{eff}) \exp\left(\frac{-U}{kT}\right) \quad (16)$$

The density of sources $\rho(\sigma_{eff})$ decreases for increasing creep strain. Eq (16) indicates that the creep rate decreases with increasing strain.

6. Constitutive modelling of low temperature creep in irradiated materials

The constitutive modelling is playing an important role in the understanding of fundamental mechanisms governing microstructural evolution in materials subjected to irradiation at extremely low temperatures. The efforts to develop validated methodologies capable of predicting microstructural evolution and mechanical property changes have been hampered by problems associated with the physical understanding of radiation in the cryogenic conditions. These challenges are ultimately caused by the highly non-linear nature of scale-dependent processes and by the limited understanding of their interactions. It has to be clearly emphasised that in the available literature there is a lack a constitutive description of the thermo-mechanical property changes of the solid materials subjected to irradiation at extremely low temperatures. Available literature models describe materials subjected to irradiation at elevated temperatures. One of them is a constitutive model for irradiated materials proposed by Ehrlich [5]. Admittedly, changes of dislocation densities as a function of fluence was introduced, but the creep deformation was explained by the interrelation of irradiation creep and swelling. Thus, this model predicts that the temperature-dependence of irradiation creep will follow those of swelling. Unfortunately the data available do not allow to confirm such a creep behaviour. Simple irradiation creep models were reviewed by Matthews and Finnis [16]. A stress effect on interstitial loop nucleation was analysed, but the physical mechanisms that bind them remained still unknown. Ehrlich [5] analysed void growth and coalescence for irradiated FCC single crystals. Mechanical modelling of irradiation creep and application of results to the analysis of creep crack growth was proposed by Murakami and Mizuno [18].

The radiation induced defects like vacancies, interstitials, vacancy loops and interstitial loops interact with the microstructure at extremely low temperature resulting in modification of the mechanical properties of the material. The evaluation of damage generated in solids exposed to a harsh environment that combines stress, extremely low temperature, and radiation fields is a major challenge in many technological domains connected to coil cases of pool-cooled superconducting magnets for fusion reactors and cryogenic lines in the particle accelerators electronic.

In this paper the new physically based creep model for materials subjected to irradiation at extremely low temperatures has

been built. The total creep rate is expressed by the respective components corresponding to relevant physical mechanisms responsible for the irradiation creep behaviour

$$\dot{\epsilon} = \dot{\epsilon}_{LE} + \dot{\epsilon}_{DA} + \dot{\epsilon}_S \quad (17)$$

The first term $\dot{\epsilon}_{LE}$ represents the creep resulting from preferred nucleation of dislocation loops and their expansion under the mechanical loads, it is connected with SIPN. The second term $\dot{\epsilon}_{DA}$ arises from the effect of stress on the elastic interaction of a radiation induced point defects with dislocations and is connected with SIPA. The third term $\dot{\epsilon}_S$ is swelling produced by climb and glide due to the absorption of interstitials on dislocations unassisted by stress. This effect is, however, a matter of separate study.

The proposed creep model is based on the experimental estimation of concentration of lattice defects (vacancies, interstitials, vacancy loops and interstitial loops) in austenitic stainless steel as a function of damage parameter dpa (displacement per atom), and comprises the relevant kinetics of evolution of radiation induced defects under mechanical loads at cryogenic temperatures.

6.1. Creep produced by the expansion of irradiation induced dislocation loops

Irradiation leads to creation of point defects like interstitials atoms and vacancies. Both types of defects can cluster to form dislocation loops. During irradiation interstitial loops develop and evolve. The elastic incompatibility connected with interstitial atoms leads to stronger interaction of dislocations with interstitials than vacancies. Ultimately, the interstitial loops formed from cluster of interstitials develop into a dislocation structure. Finally, during irradiation, interstitial loops create stable defects in the form of dislocation loops, whereas vacancy loops are unstable.

Assumptions in mathematical modelling of low temperature creep of irradiated material

- interstitials and vacancy loops result due to irradiation
- dislocation loops evolve under mechanical loads
- motion of dislocation lines over the Peierls stress hills is the rate controlling process in creep
- Glen-Mott quantum mechanical dislocation tunneling effect allows extending the theory to the liquid helium temperature range

Creep is produced by the expansion of irradiation induced dislocation loops under mechanical loads. The creep rate is expressed by the following general equation

$$\dot{\epsilon}_{LE} = b q_l(dpa) \dot{r}(dpa, \sigma) R^2(r, \sigma, dpa) \quad (18)$$

where $q_l(dpa)$ is the density of dislocation loops, σ is applied stress, $\dot{r}(dpa, \sigma)$ is the average rate of expansion of dislocation loop of radius r , R is the average radius to which a dislocation loop expands. The measure of radiation damage in the solid is displacements per atom (dpa). The density of dislocation loops and the average size plotted against irradiation dose are obtained experimentally by Courcelle et al. [3] from observations of dislocation networks and dislocations dynamics simulation. Distribution of the density of dislocation loops and mean diameter is shown in Fig. 15.

A power function reflect dependence between the density of dislocation loops and the dpa variable, reads

$$q_l = \begin{cases} C_1(dpa)^{n_1} & \text{for } dpa < D_s \\ C_2(dpa)^{n_2} & \text{for } dpa \geq D_s \end{cases} \quad (19)$$

In the vicinity of threshold value D_s , further evolution of dislocation loops size ceases (cf. [20]). The average dislocation loop radius r is expressed by

$$r = \begin{cases} C_r(dpa)^{n_r} & \text{for } dpa < D_s \\ r_0 & \text{for } dpa \geq D_s \end{cases} \quad (20)$$

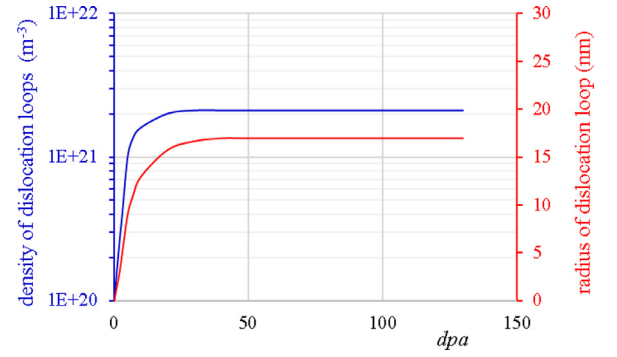


Fig. 15. Number of density of dislocation loops and mean diameter as a function of irradiation dose (for austenitic stainless steel, based on Courcelle et al. [3]).

where C_1 , C_2 and C_r are the material parameters. The rate of expansion of a dislocation loop can be calculated using the mechanism of development the velocity of a dislocation line over Peierls stress hills. The rate of expansion of a dislocation loop of radius r is

$$\dot{r}(\sigma, dpa) = \left(\frac{vr(\sigma, dpa)a}{b} \right) \exp\left(-\frac{U}{kT}\right) \quad (21)$$

where a is the distance between Peierls hills. Seeger [25] stated that the dislocation line moves over the Peierls hill not as a whole rather in small parts. The activation energy Eq. (13) and the frequency of vibration of a dislocations loop Eq. (14) is adopted according to Weertman's theory.

Assuming that the quantum tunneling mechanism is responsible for creep deformation the temperature-dependent term $\exp(-U/kT)$ is replaced by the term expressed the tunneling probability expressed by Eq. (9). The rate of expansion of a dislocation loop takes the form

$$\dot{r}(\sigma, dpa) = \left(\frac{vr(\sigma, dpa)a}{b} \right) \exp\left(\frac{-\beta\mu}{\sigma}\right) \quad (22)$$

Integration Eq. (22) allows obtaining the average radius to which a dislocation loop expands under tension

$$R(\sigma, dpa) = r(dpa) \exp\left(\left(\frac{va}{b}\right) \exp\left(\frac{-\beta\mu}{\sigma}\right) t\right) \quad (23)$$

Expansion of the average radius of a dislocation loop under stress is shown in Fig. 16.

The average radius of a dislocation loop evolution under tension as a function of time show exponential response. The higher value of tunneling probability significantly accelerates the dislocation loop size (Fig. 16a). The initial value of radiation defects is obvious (Fig. 16b).

The critical value of radius of dislocation loop, at the moment of rupture, is designated by r_c . Substituting Eq. (23) into Eq. (18) one obtains the creep rate produced by the expansion of dislocation loops

$$\dot{\epsilon}_{LE} = q_l v a \exp\left(\frac{-\beta\mu}{\sigma}\right) r^3 e^{t\left(\frac{va}{b}\right) \exp\left(\frac{-\beta\mu}{\sigma}\right)} \quad (24)$$

The creep rate behaviour predicted by Eq. (24) is reported in Fig. 17. Immediately, after application of load some nonzero creep rate $\dot{\epsilon}_0$ resulting from the evolution of radiation induced dislocation loops is observed.

The creep deformations observed at extremely low temperatures are instantly after applying loads proportional to $\exp(t)$. This is known as a primary creep. The primary creep is of fundamental importance in the engineering applications because it makes it possible to include the work-hardening processes occurring at

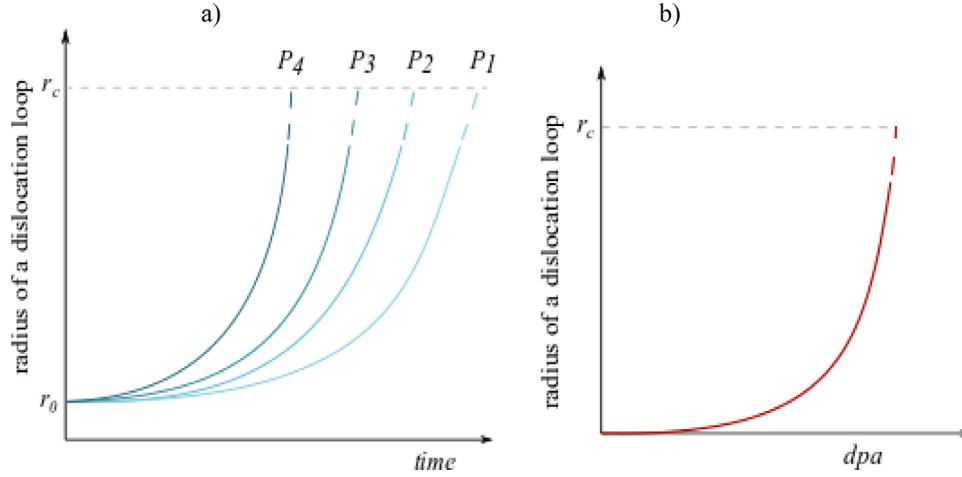


Fig. 16. Predicted expansion of average radius of a dislocation loop under stress a) for different tunneling probability values ($P_1 < P_2 < P_3 < P_4$) as a function of time b) as a function of dpa .

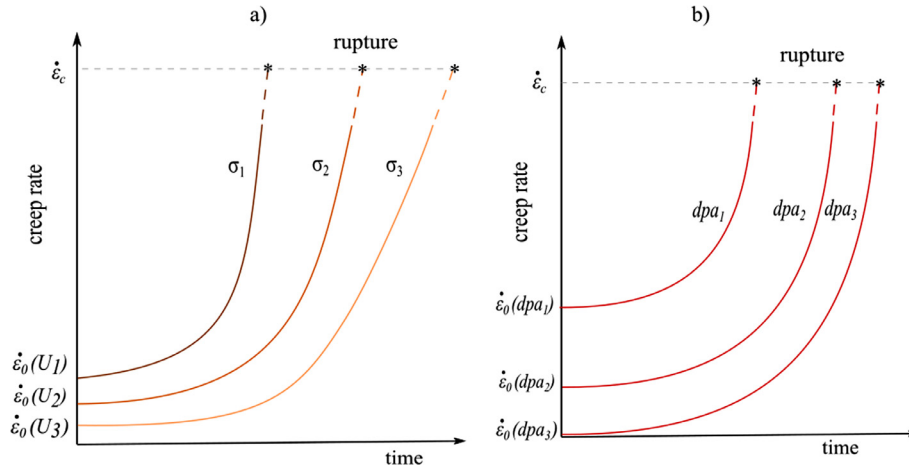


Fig. 17. Predicted creep rate behaviour produced by the expansion of irradiation induced dislocation loops a) as a function of stresses ($\sigma_1 > \sigma_2 > \sigma_3 > \sigma_4$) b) for different dpa ($dpa_1 > dpa_2 > dpa_3$).

extremely low temperature. In the primary creep stage, the creep rate changes with time. In the secondary creep stage, it can be expected that the creep strain rate stabilizes at a constant value, and the creep strain becomes linear function of time. Similar effect was observed by Yen et al. [35] during the tests of materials carried out at extremely low temperatures. The creep strain rate reaches a constant value. Finally, during the last third stage the creep rate starts to increase rapidly, which inevitably leads to creep rupture. The critical value of creep rate is designated by $\dot{\epsilon}_c$. In order to estimate the lifetime of the components controlled by the creep rupture, the key issue is analysis of the behavior of tertiary creep. The secondary and tertiary creep of materials at extremely low temperatures has not been explained here due to fact, that there was lack of experimental data related to long-time creep tests at cryogenic temperatures.

Experimental tests of irradiated materials at cryogenic temperatures are complicated, laborious, time consuming, expensive, and require advanced experimental equipment. For this reason, there is a lack of such tests, and there is no set of creep data for irradiated metals used at cryogenic temperatures. Therefore, the experimental validation of the proposed constitutive model for irradiated materials at extremely low temperature at this point is not possible. Integrating Eq. (24) with respect to time allows to obtain the expression for creep rate

$$d\epsilon_{LE} = \int q_1 \nu a r^3 e^{-\frac{\beta\mu}{\sigma}} e^{\left(\frac{\nu a}{b}\right)e^{-\frac{\beta\mu}{\sigma}} t} dt \quad (25)$$

Using the relations: $e^x = \sum_{n=0}^{\infty} \frac{(x)^n}{n!}$ and $e^{-x} = \sum_{n=0}^{\infty} \frac{(-x)^n}{n!} = \sum_{n=0}^{\infty} \frac{e^{inx}}{n!}$ the integral expression in Eq. (25) is defined by the following power series

$$e^{\left(\frac{\nu a}{b}\right)e^{-\frac{\beta\mu}{\sigma}} t} = \sum_{n=0}^{\infty} \frac{\left(\frac{\nu a}{b}\right)^n e^{-\frac{\beta\mu}{\sigma} t}}{n!} \quad (26)$$

Finally, Eq. (25) takes the form

$$d\epsilon_{LE} = q_1 \nu a r^3 e^{-\frac{\beta\mu}{\sigma}} \int e^{\left(\frac{\nu a}{b}\right)e^{-\frac{\beta\mu}{\sigma}} t} dt = q_1 \nu a r^3 e^{-\frac{\beta\mu}{\sigma}} \sum_{n=0}^{\infty} \frac{\left(\frac{\nu a}{b}\right)^n}{n!} \int e^{-\frac{\beta\mu}{\sigma} t} e^{n\left(\frac{\nu a}{b}\right)e^{-\frac{\beta\mu}{\sigma}} t} dt \quad (27)$$

Finally, the creep strain takes the form

$$\epsilon_{LE} = q_1 \nu a r^3 e^{-\frac{\beta\mu}{\sigma}} \sum_{n=0}^{\infty} \frac{\left(\frac{\nu a}{b}\right)^n}{n!} \left(-\frac{\sigma}{n\beta\mu} e^{-\frac{n\beta\mu}{\sigma} t} + C_\epsilon \right) \quad (28)$$

where C_ϵ is constant parameter. In the liquid helium temperature range the application of Eqs. (24) and (28) leads to difficulties. In these temperatures these equations predict that creep strain will occur for stress close to the Peierls stress. The experimental results for unirradiated materials indicated appreciable creep at moderate stresses in this temperature range [22,35]. One might expect that for irradiated materials the creep strain will be even greater.

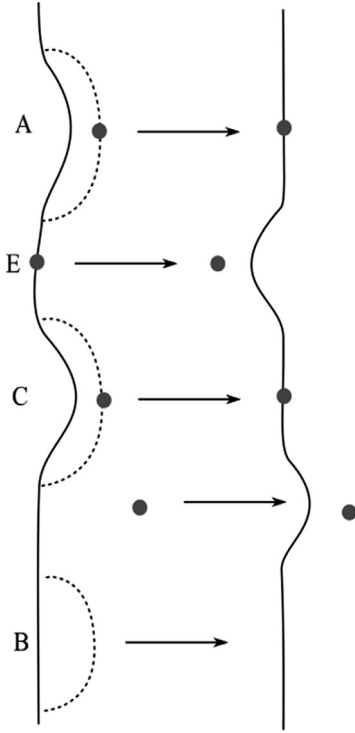


Fig. 18. The motion of a dislocation line with the aid of interaction of radiation induced point defects with existing dislocations in materials.

6.2. Creep produced by the elastic interaction of a radiation induced point defects with existing dislocations in materials

The following section presents the constitutive model of creep appropriate for metals cooled to cryogenic temperatures subjected to radiation and constant stress amplitude. Here, creep arises from the effect of stress on the elastic interaction of a radiation induced point defects with existing dislocations in materials. There are a large number of interstitial atoms and cavities in irradiated materials which can interact with existing dislocations employing Peierls energy in their immediate neighbourhood. The course of this process is illustrated in Fig. 18. Interstitial atoms exert an attractive force on a dislocation line which is not quite large enough to pull a dislocation jog over into the next Peierls valley. Lastly, it should be taken into account that not all the irradiation points defect exert the same attractive or repulsive force on a dislocation. Formation of a jog at point B requires the larger activation energy than at points A and C.

Some of point defects have a strong enough force to pull a dislocation jog over the Peierls hill. For the impurity atom located at point E the dislocation line does not break as a result of expanding two jogs A and C. Thus the Peierls energy may be reduced in the presence of interstitial atom to a value much smaller than activation energy of creep at intermediate temperatures. But creep activation energy at temperatures well above the liquid helium range is not necessarily reduced [34].

The creep rate resulting from interaction of a radiation induced point defects with existing dislocations in materials is expressed by the following general equation

$$\dot{\varepsilon} = q_d(dpa) \frac{dx}{dt}(\sigma) \mathcal{L}^2 \quad (29)$$

where $q_d(dpa)$ is the density of radiation induced point defects, σ is applied stress, dx/dt is the velocity of motion of a dislocation segment, \mathcal{L} is the average distance to which a dislocation line relocate. The velocity of motion of a dislocation segment under applied

stress is proposed in the form

$$\frac{dx}{dt} = \frac{\nu La}{b} \exp\left(\frac{-\beta\mu}{\sigma}\right) \quad (30)$$

where ν the frequency of vibration of a dislocation line, L denotes a length of dislocation segment, a is the distance between Peierls hills.

Finally, the creep rate takes the form

$$\dot{\varepsilon} = q_d(dpa) \frac{\nu La}{b} \exp\left(\frac{-\beta\mu}{\sigma}\right) \mathcal{L}^2 \quad (31)$$

In the range cryogenic temperatures irradiated defects and other impurities are extremely important since they may permit tunneling and thus give rise to Glen-Mott type creep and, paradoxically, soften a crystal by permitting dislocation motion at stresses well below the Peierls stress.

7. Constitutive modelling of low temperature creep in unirradiated materials

The following section presents the constitutive model responsible for creep in metals cooled to cryogenic temperatures subjected to constant stress amplitude are considered. The starting point is the assumption that the creep rate may be described as a product of two separate functions of stress and temperature

$$\dot{\varepsilon}^c = f_\sigma(\sigma) f_T(T) \quad (32)$$

The commonly used functions of stress are:

× power law

$$f_\sigma(\sigma) = \dot{\varepsilon}_0 \left(\frac{\sigma}{\sigma_0}\right)^n \quad (33)$$

× exponential law

$$f_\sigma(\sigma) = \dot{\varepsilon}_0 \exp\left(\frac{\sigma}{\sigma_0}\right) \quad (34)$$

× hyperbolic sine law

$$f_\sigma(\sigma) = \dot{\varepsilon}_0 \sinh\left(\frac{\sigma}{\sigma_0}\right) \quad (35)$$

where $\dot{\varepsilon}_0$ is the reference creep rate, σ_0 is the reference stress and n is a material constant. The dependence on the temperature is usually expressed by the Arrhenius law

$$f_T(T) = \exp\left(-\frac{U}{kT}\right) \quad (36)$$

The constitutive relation for the creep rate in metals cooled to cryogenic temperatures is adopted in the following form

$$\dot{\varepsilon}^c = A \exp\left(-\frac{U}{k_B T}\right) \exp(B(\sigma - h\varepsilon^c)) \quad (37)$$

where ε is the creep strain, $\dot{\varepsilon}$ the creep rate, σ the stress, A and B are constants, k is Boltzmann's constant, T the absolute temperature, U is activation energy, and h is the coefficient of strain hardening ($h=d\sigma/d\varepsilon$). It is important that the temperature does not enter into the exponential stress term in Eq. (40) and the activation energy does not depend on temperature.

Separation of variables allows one to solve Eq. (37)

$$\frac{d\varepsilon^c}{\exp(B(\sigma - h\varepsilon^c))} = A \exp\left(-\frac{U}{k_B T}\right) dt \quad (38)$$

Eq. (38) is simplified by substituting $x = \sigma - h\varepsilon^c$ and $d\varepsilon^c = -dx/h$.

$$\int \frac{-dx}{h \exp(Bx)} = \int A \exp\left(-\frac{U}{k_B T}\right) dt \quad (39)$$

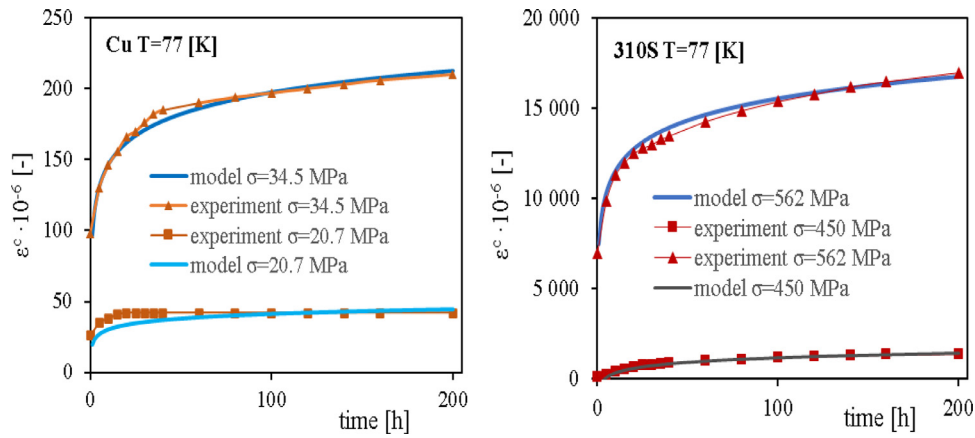


Fig. 19. A) Numerical model versus experiment for Cu at 77K for two levels of loads $\sigma=20.7$ MPa and $\sigma=34.5$ MPa B) Numerical model versus experiment for 310S at 77K for two levels of loads $\sigma=450$ MPa and $\sigma=562$ MPa.

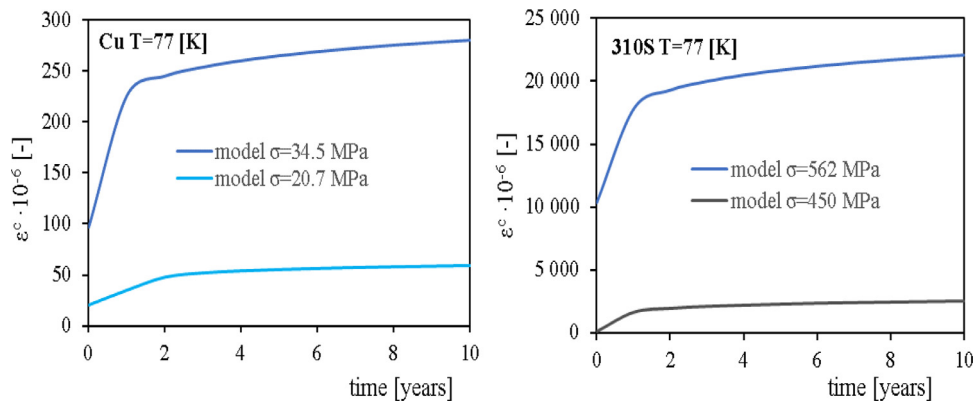


Fig. 20. Creep strain for based on the model a) for Cu at 77K for two levels of loads $\sigma=20.7$ MPa and $\sigma=34.5$ MPa b) for 310S at 77K for two levels of loads $\sigma=450$ MPa and $\sigma=562$ MPa.

Table 1

Material parameters.

parameters	parameters values
U_0	0.02 [eV] (Mott [17])
h	130 [GPa] for Cu [35], 196 [GPa] for 310S [22]
σ_0	$\sigma_0=38.5$ [MPa] for Cu at $T=77$ [K] [35] $\sigma_0=248$ [MPa] for 310S at $T=293$ [K] [22] $\sigma_0=562$ [MPa] for 310S at $T=77$ [K] [22] $\sigma_0=783$ [MPa] for 310S at $T=4$ [K] [22]
k	8.617×10^{-5} [eV/K]
a	3–5 atomic distances (Kamimura [10])
σ_p	1.4 [MPa] (Kamimura [10])
μ	25 [GPa] (Al; Kamimura [10])
ν	10^{11} - 10^{12} [Hz] (Mott [17])

Integrating both sides of Eq. (39) one obtains the logarithmic creep equation

$$\varepsilon^c = \frac{\sigma}{h} + \frac{1}{Bh} \ln \left(ABh \exp \left(-\frac{U}{k_B T} \right) t \right) \quad (40)$$

The quantum mechanical tunneling phenomenon is proposed to explain the creep at extremely low temperature for unirradiated materials. The activation energy is adopted according to Glen-Mott model Eq. (5). The parameters needed to estimate the profile of creep rate according to Eq. (31) are given in Table 1.

The creep behaviour predicted by the model is reported in Fig. 19. Comparison of the creep curves between the experimental results and the numerical simulations for copper at 77K for two levels of loads $\sigma=20.7$ MPa and $\sigma=34.5$ MPa (Fig. 19a) and

for stainless steel at 77K for two levels of loads $\sigma=450$ MPa and $\sigma=562$ MPa (Fig. 19b) are shown.

The numerically obtained creep curves were imposed on the experimental data in order to verify their consistence. The good agreement between the numerical simulations and the experiments indicates that the developed constitutive model can be recommended in the creep behaviour evaluation of materials at extremely low temperatures. Using the constitutive model (Eq. 41) the creep deformation over an extended period is shown in Fig. 20. The numerical predictions incorporating the creep curve show a logarithmic increase of creep deformation.

Conclusion

The purpose of this paper is to devise and characterize physically-based constitutive model which allow to describe the effects of creep of irradiated materials at cryogenic temperatures and the physics of defect generation. The quantum tunneling as the mechanism responsible for creep deformations at sufficiently low temperatures (liquid nitrogen 77 K, liquid helium 4.2 K) and relatively high-stress levels is adopted. Dislocations that are locally pinned can escape from their pinning points more rapidly via tunneling than by means of thermal activation. The outcome of this paper provides an insight into the physical mechanisms underlying low temperature creep of irradiated materials effect. Peierls lattice resistance mechanism is used to explain creep produced by the elastic interaction of a radiation induced point defects with existing dislocations in materials. This mechanism is based on the hypothesis that dislocation can pass through barriers (interstitials

atoms and cavities) when corresponding Peierls energy is reached. Thus, in this case, the activation energy may be reduced in the presence of interstitial atom to a value much smaller than activation energy of creep at intermediate temperatures. Furthermore, assuming the quantum tunneling mechanism the kinetic law for evolution of irradiation induced dislocation loops is proposed. Predicted creep rate behaviour as a function of stresses and dpa are presented. While the tunneling based model correlation showed consistency with the limited data at 77 K, this was for the unirradiated material. The proposed model for effects of irradiation on creep in the cryogenic range could not be verified due to lack of data.

Declaration of Competing Interest

The authors declare that they have no known competing financial interests or personal relationships that could have appeared to influence the work reported in this paper.

Appendix: The tunneling probability

Gilman's derivation [6] for the tunneling probability (Eq. 8) and it's simplification (Eq. 9) are given in this Appendix.

Gilman [6] proposed the simple but appropriate form of potential of local elastic interaction of dislocation with point defect in the form

$$H(x) = -H_0(1 + |x|)e^{-|x|} \tag{A1}$$

where H_0 is the total energy per unit length and x stands for a displacement of the centre of dislocation

$$x = z/\delta \tag{A2}$$

δ denotes the range of the potential, z is the displacement of dislocation. This potential expresses a linear restoring force for small displacements and decays like a wave function for large x

$$F(x) = -\frac{\partial H}{\partial x} = -H_0|x|e^{-|x|} \tag{A3}$$

Also, this force is symmetric about $x=0$ for small x and this reaches its maximum magnitude when $x=1$ or $z=\delta$.

The force caused by the applied stress σ takes the form

$$F = -\sigma b^2 \tag{A4}$$

Thus, the potential energy associated with a displacement of the dislocation segment is expressed in the form

$$V(x) = -\sigma b^2 \delta x \tag{A5}$$

In light of the above, the total energy of the system takes the form

$$H(x) = -H_0(1 + x)e^{-x} - \sigma b^2 \delta x \tag{A6}$$

The proposed approach shows that two positions exist which have the same energy. Thus the dislocation segment can tunnel from $x=0$ to $x=x^*$.

For $x=x^*$ the total energy is

$$H_0 = \sigma b^2 \delta x^* \tag{A7}$$

which leads to the relation

$$x^* = \frac{H_0}{b^2 \delta \sigma} \tag{A8}$$

In Fig. 1A the potential of interaction of dislocation is sketched together with the driving potential that results from the applied stress.

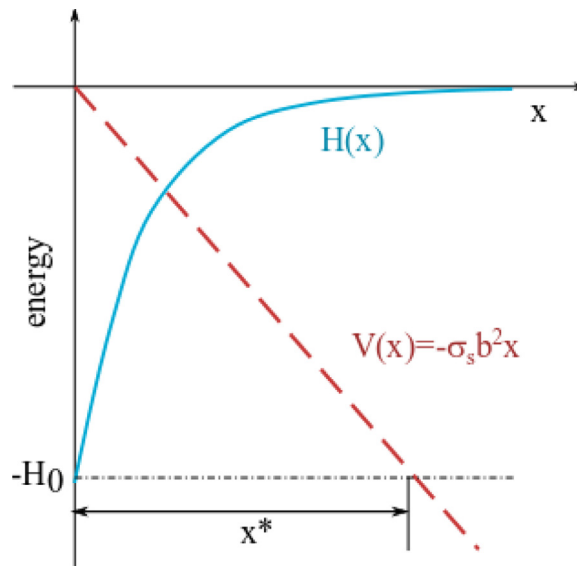


Fig. 1A. Energy configuration for a short segment of a bound dislocation

In order to estimate the tunnelling probability the wave equation with a periodic potential energy is expressed in the following form

$$\psi_k(x) = e^{ikx} H_k(x) \tag{A9}$$

The condition that ψ_k should remain finite all values of x imposes the restriction that k be real. The wave equation for dislocation with energy $H(x)$ is defined as follows

$$\left\{ \frac{h^2}{8\pi^2 m} \frac{\partial^2}{\partial x^2} + H(x) \right\} \psi(V(x), x) = 0 \tag{A10}$$

An approximate solution of this equation may at once be obtained if one observes that the term $V(x)$ changes only slightly in the distance of a single lattice constant. Such solution is

$$\psi(V(x), x) = e^{i \int K dx} H_k(x) \tag{A11}$$

With a given $V(x)$, K is real only for certain values of x . K is defined as follows

$$K = \xi(x) + i\eta(x) \tag{A12}$$

where $\xi(x)$ is the real part and $\eta(x)$ is the imaginary part, i represents the imaginary unit. Specifically, if the wave function is given in the range BC the transition probability P is given by

$$P = \left| \frac{\psi(x_C)}{\psi(x_B)} \right|^2 \tag{A13}$$

Finally, transition probability takes the form

$$\left| \frac{\psi(x_C)}{\psi(x_B)} \right|^2 \simeq e^{-\int_B^C \eta(x) dx} \tag{A14}$$

Using the equations (A10-A14) Gilman [6] derived the probability of tunneling as

$$P = \exp\left(\frac{-mH_0^2}{4\hbar^2 \sigma b}\right) \tag{A15}$$

where m denotes an effective mass of moving dislocation (atomic mass per atomic plane cut by it [17]). Eq (A15) was further simplified by Gilman by using several assumptions and approximations including: (a) the total binding energy H_0 per unit length of dislocation is proportional to the shear modulus μ and square of b the Burgers vector

$$H_0 \simeq \mu b^2 \tag{A16}$$

and (b) the effective-mass can be approximated using density as

$$m \simeq \rho b^3 \quad (\text{A17})$$

Using relations (A15) through (A17), and identifying a relation between local oscillator frequency and binding energy, Gilman [6] gave the following expression for the probability of motion

$$P = \exp\left(\frac{-\beta\mu}{\sigma}\right) \quad (\text{A18})$$

where β is a coefficient which can be found from experiments.

CRedit authorship contribution statement

Aneta Ustrzycka: Conceptualization, Methodology, Investigation, Visualization, Writing - original draft, Writing - review & editing.

References

- [1] R.J. Arsenault, An investigation of the mechanism of thermally activated deformation in tantalum and tantalum-base alloys, *Acta Metallurgica* 14 (1966) 831–838.
- [2] J. Betten, *Creep mechanics*, Springer, Berlin Heidelberg New York, 2002.
- [3] A. Courcelle, C. Bisor, E. Piozin, M. Kountchou, P. Gavaille, M. Le Flem, J.-L. Séran, Evolution under Irradiation of Optimized Austenitic Steel For Gen-IV Reactors, Impact on Fuel Cladding Properties and Performances 115 (2016) 04003 2nd Int. Workshop Irradiation of Nuclear Materials: Flux and Dose Effects.
- [4] A.H. Cottrell, Logarithmic and Andrade creep, *Philosophical Magazine Letters* 75 (1997) 301–308.
- [5] K. Ehrlich, Irradiation creep and interrelation with swelling in austenitic stainless steels, *Journal of Nuclear Materials* 100 (1981) 149–166.
- [6] J.J. Gilman, Escape of Dislocations from Bound States by Tunneling, *Journal of Applied Physics* 39 (1968) 6086.
- [7] J.W. Glen, The creep of cadmium crystals at liquid helium temperatures, *Philosophical Magazine* 1 (5) (1956) 400–408.
- [8] N. Karanjaokar, F. Stump, P. Geubelle, I. Chasiotis, A thermally activated model for room temperature creep in nanocrystalline Au films at intermediate stresses, *Scripta Materialia* 68 (2013) 551–554.
- [9] M.E. Kassner, K. Smith, Low temperature creep plasticity, *Journal of Material Science and Technology* 3 (2014) 280–288.
- [10] Edagawa K. Kamimura Y., S. Takeuchi, Experimental evaluation of the Peierls stresses in a variety of crystals and their relation to the crystal structure, *Acta Materialia* 61 (2013) 294–309.
- [11] M.E. Kassner, K. Smith, C.S. Campbell, Low-temperature creep in pure metals and alloys, *Journal of Material Science and Technology* 50 (2015) 6539–6551.
- [12] G.H. Kinchin, R.S. Pease, The displacement of atoms in solids by radiation, *Reports on Progress in Physics* 18 (1955) 1–52.
- [13] V.A. Koval, A.I. Osetskii, V.P. Soldatov, V.I. Startsev, Temperature Dependence of Creep in F.C.C. and H.C.P. Metals at Low Temperature *Advances in Cryogenic Engineering* (1978) 249–255.
- [14] P.R. Landon, J.L. Lytton, L.A. Shepard, J.E. Dorn, The activation energies for creep of polycrystalline copper and nickel, *Trans ASM* 51 (1959) 900–910.
- [15] P. Lutkiewicz, B. Skoczeń, C. Garion, Micro-damage propagation in ultra-high vacuum seals, *International Journal of Pressure Vessels and Piping* 87 (2010) 187–196.
- [16] J.R. Matthews, M.W. Finnis, Irradiation creep models – an overview, *Journal of Nuclear Materials* 159 (1988) 257–285.
- [17] N.F. Mott, Creep in metal crystals at very low temperatures, *Philosophical Magazine* 1 (6) (1956) 568–572.
- [18] S. Murakami, M. Mizuno, Mechanical modelling of irradiation creep and its application to the analysis of creep crack growth. *Creep in Structures*, IUTAM Symposium Cracow/Poland Springer-Verlag Berlin Heidelberg, 1991.
- [19] F.R.N. Nabarro, Thermal activation and Andrade creep, *Philosophical Magazine Letters* 75 (1997) 227–233.
- [20] N. Nita, R. Schaeublin, M. Victoria, Impact of irradiation on the microstructure of nanocrystalline materials, *Journal of Nuclear Materials* 1 (2004) 329–333.
- [21] K. Nordlund, S.J. Zinkle, A.E. Sand, F. Granberg, R.S. Averback, R. Stoller, T. Suzudo, T.L. Malerba, F. Banhart, W.J. Weber, F. Willaime, S.L. Dudarev, D. Simeone, Improving atomic displacement and replacement calculations with physically realistic damage models, *Nature Communications* 9 (2018) 1084.
- [22] T. Ogata, O. Umezawa, K. Ishikawa, Low temperature creep behavior of stainless steels, *Advances in Cryogenic Engineering* 36 (1990) 1233–1239.
- [23] A.I. Osetskii, V.P. Soldatov, V.I. Startsev, V.D. Natsik, Temperature dependence and activation parameters of creep in Zn in the temperature range 1.5 to 80 K, *Physica Status Solidi A* 22 (1974) 739–748.
- [24] L.D. Roth, A.E. Manhardt, E.N.C. Dalder, R.P. Kershaw Jr, Creep of 304LN and 316L stainless steels at cryogenic temperatures, *Advances in Cryogenic Engineering* 32 (1986) 369–376.
- [25] A. Seeger, H. Donth, F. Pfaff, The Mechanism of Low Temperature Mechanical Relaxation in Deformed Crystals *Discussions of the, Faraday Society* 23 (1957) 19–30.
- [26] B. Skoczeń, *Encyclopedia of Continuum Mechanics Creep at Extremely Low Temperatures*, Springer, 2018.
- [27] B. Skoczeń, A. Ustrzycka, Kinetics of evolution of radiation induced micro-damage in ductile materials subjected to time-dependent stresses, *International Journal of Plasticity* 80 (2016) 86–110.
- [28] K. Szuwalski, A. Ustrzycka, Optimal design of bars under nonuniform tension with respect to mixed creep rupture time, *International Journal of Non-Linear Mechanics* 47 (2012) 55–60.
- [29] K. Szuwalski, A. Ustrzycka, The influence of boundary conditions on optimal shape of annular disk with respect to ductile creep rupture time, *European Journal of Mechanics A-Solids* 37 (2013) 79–85.
- [30] J. Tabin, B. Skoczeń, J. Bielski, Strain localization during discontinuous plastic flow at extremely low temperatures, *International Journal of Solids and Structures* 97–98 (2016) 593–612.
- [31] J.K. Tien, C-T. Yen, Cryogenic Creep of Metals, *Advances in Cryogenic Engineering Materials* (1984) 319–338.
- [32] B. Ustrzycka Skoczeń, M. Nowak, Kurpaska Ł., E. Wyszowska, J. Jagielski, Elastic-plastic-damage model of nano-indentation of the ion-irradiated 6061 aluminium alloy, *International Journal of Damage Mechanics* 29 (2020) 1271–1305.
- [33] D.O. Welch, R. Smoluchowski, Exhaustion theory of creep metals at low temperatures, *Journal of Physics and Chemistry of Solids* 33 (1972) 1115–1127.
- [34] J. Weertman, Dislocation model of low-temperature creep, *Journal of Applied Physics* 29 (1958) 1685–1989.
- [35] C. Yen, T. Caulfield, L.D. Roth, J.M. Wells, J.K. Tien, Creep of copper at cryogenic temperatures, *Cryogenics* 24 (1984) 371–37.
- [36] M. Życzkowski, Optimal structural design under creep conditions, *Applied Mechanics Reviews* 12 (1988) 453–461.